LABORATORY STUDY OF MECHANICAL AND THERMODYNAMIC PROPERTIES OF ANALOG LUNAR POLAR CRATER ICE-REGOLITH MIXTURES.

J. Behrens[1], K. Zacny[2], T. Prettyman[3], M.E. Landis[3], J. Atkinson[2], Z. Siyed[4], [1]The Boeing Company, El Segundo, CA, [2]Honeybee Robotics, Pasadena, CA, [3]Planetary Science Institute, Albuquerque, NM, [4]The Boeing Company, Huntington Beach, CA. (john.w.behrens@boeing.com).

Introduction: Direct confirmation of the presence of water by the Lunar CRater Observation and Sensing Satellite (LCROSS) [1] strongly motivates in situ exploration of the polar cold traps to determine its origins and to determine whether the volatiles contained in the deposits would be of value as a resource [2].

Understanding the thermophysical properties of lunar soil is required before sending exploratory landers/rovers with drills or any other sample-acquisition instruments, especially into the permanently shadowed polar regions, where both dry soil and ice are expected. Understanding the properties of icy soil at cryogenic temperatures (35-50 K) is important from a scientific standpoint (e.g., assessing ice stability) and also in determining how a proposed excavation operation would thermally alter the deposit.

We present results characterizing the mechanical and thermodynamic properties of icy regolith, using JSC-1a (mare) and NU-LHT-2M (highland) lunar simulants with varying water content in a vacuum chamber between 35-50 K, similar to temperatures found in permanently shadowed lunar craters [3].

Unconfined Compressive Strength Testing: We obtained Unconfined Compressive Strength (UCS) measurements of compacted JSC-1a samples at water contents of 3%, 5%, and 12% (by mass), as well as high-resolution stress-strain curves, at temperatures of 253 K and 77 K. The results allow for the determination of the material strengthening at low temperatures and brittle-to-ductile failure mode transitions.

Samples of icy JSC-1a were prepared by a three-step procedure: (1) compaction and freezing of moist simulant mixtures, (2) cutting and shaping of frozen mixtures into testing cylinders, and (3) storage of shaped samples. While moisture content was determined prior to freezing, sample density was calculated both before the freezing process (during compaction) and after the sample had been cut to length, providing two measurements of bulk density. Unconfined uniaxial compressive tests under constant displacement rates (0.24 mm/s to 2 mm/s) were conducted on a specialized mechanical testing machine designed to operate in a vacuum and at cryogenic temperatures.

Force and displacement data were recorded as voltages and converted to MPa and mm (respectively) using calibration curves determined prior to experimentation. Strain corrections, due to the finite stiffness of the apparatus and generally only significant at higher loads, was estimated and removed in post-processing of the data.

Force and displacement curves versus time were the final processed data products, with time acting as a proxy for displacement when plotted against force due to the constant rate. After compression, the sample was removed from the cooling container and immediately photographed. The force (stress) displacement curves, along with the images, are used to determine the peak stress and the deformation mechanisms present.

An example stress curve at 0.24 mm/s and 253 K (5% moisture content) is shown in Figure 1. The red curve is the axial stress imparted by the press onto the sample, while the green curve is the calculated inelastic strain. Inelastic strain was calculated by estimating elasticity of the sample and apparatus proportional to the axial force imparted by the apparatus and removing it from the measured strain curve. The curve can be split into four regions: (I) the closure of favorably-oriented microcracks in the sample and coupling of the sample to the platen upon initial compression, (II) a linearly elastic region, (III) yielding of the sample and development of distributed fractures, and (IV) failure of the sample and strain-weakening to a plastic limit.

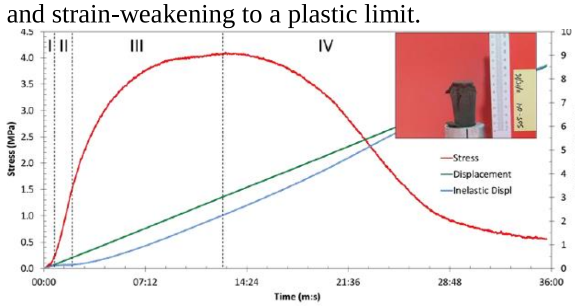

Figure 1. JSC-1a Sample stress & strain curve

Thermodynamic Testing: To determine the thermodynamic properties of icy lunar regolith simulant at cryogenic temperatures, we designed an experiment to test the heat capacity (C_P) and conductivity (k) of ice-cemented regolith simulant samples. An Ilikon vacuum chamber with a liquid nitrogen shroud was used for the testing with an 18” box helium cryostat mounted to one end dome. When wrapped with 10 layer MLI, the cryostat could consistently achieve wall temperatures below 50 K with minimal liquid nitrogen boil-off from the shroud.

A test sample preparation method similar to that used for the UCS testing was developed. Water and regolith simulant were weighed and mixed and then packed into a 1” thick by 1” diameter plastic tube and placed in a freezer. Once frozen, the samples were removed from the freezer and prepared for testing. Silicon temperature diodes were placed at both ends of the sample and a heater element placed at one end. The assembly was then wrapped in 20 layers of MLI and placed on the floor of the cryostat.

After chamber pump-down, the cryostat was started, usually requiring 24-36 hours for the samples to reach test temperatures. Once at temperature, the test was started by applying power to the top of the sample. We recorded the change in temperature with time and the final equilibrium temperature of the sample. The power was then removed and the temperature decay rate and final cold equilibrium temperature were documented.

Testing was done on both JSC-1a and NU-LHT-2M simulant with moisture contents of 3%, 5% and 12%. An example test curve is provided in Figure 2.

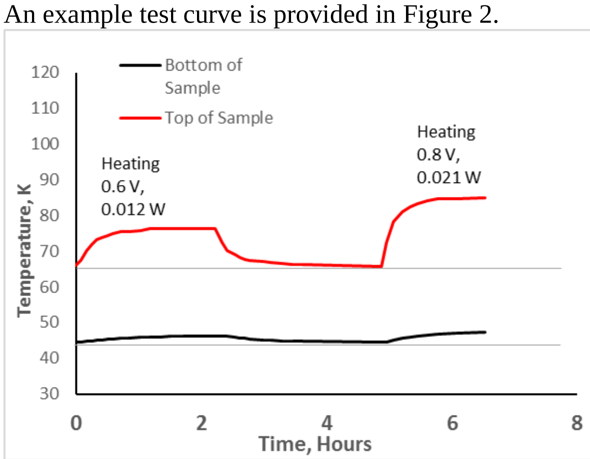

Figure 2. Test results for JSC-1a with 5% moisture content

Test results analysis: The peak unconfined compressive strengths of the samples as a function of temperature are presented in Figure 3. As the strength of JSC-1a has no appreciable temperature sensitivity, any additional strength at lower temperatures is expected to be due to the strengthening of ice [4]. Higher ice saturations (12%) are therefore expected to show increased strengthening compared to the lower saturation (3%) samples.

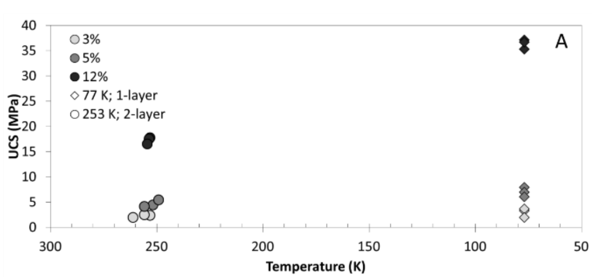

Figure 3. UCS of icy JSC-1a samples as a function temperature

Analyses of the thermal data were carried out using an axial heat flow model. Thermal conductivity was determined given heater power and the temperature increase across the sample with the heater on. Heat capacity was determined from the time-dependent decrease in the temperature drop following removal of heater power by using a model to fit the results, as shown in Figure 4.

The temperature at the moment the power to the sample is turned off is key to constraining the uncertainty in C_P. For example, Figure 4 shows a variety of cooling curves calculated with varying C_P and the k previously calculated for that sample. Depending on how we weight the first data point after the heater has been turned off, a range of C_P are possible with close fits to the data.

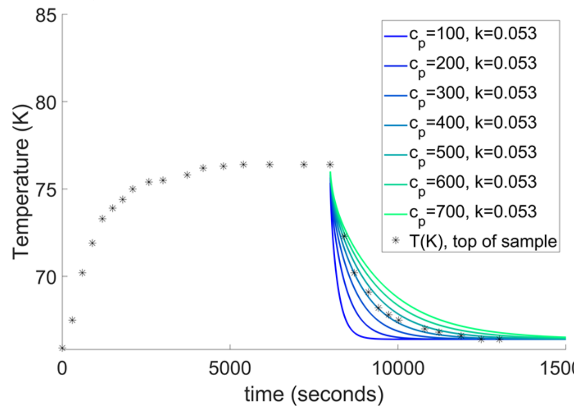

Figure 4. Experimental data plotted with model cooling curves

Future Work: We are on track to complete testing of samples in the cryo-chamber and will calculate the k and C_P of the ice/JSC-1a and ice/NU-LHT-2M mixtures. We will show how thermal properties are affected by ice content at low temperatures. Experimental results will be compared to models and other data sets. The thermo-mechanical properties determined by this study will be used to assess the efficacy of prospective operations for in situ extraction of volatiles within lunar permanently shadowed craters for scientific studies and resource utilization.

References: [1] Colaprete A. et al. (2010), Science, 330, 6003, 463-468. [2] Jolliff, B. et al., (2007) Report from Lunar Exploration and Science Workshop, p. 30, Feb. 2007,. [3] Williams, J. P. et al. (2017) *Icarus* 10.1016/j.icarus/2016.08.012. [4] Kirby, S. H. et al. J. Phys., C1(3), 227–232.

Acknowledgements: This work was supported by NASA via the ROSES LASER program, contract NNH14CK96C